MCS OBSERVATIONS OF THE WEATHER AND CLIMATE OF MARTIAN NORTHERN SPRING AND SUMMER

D. M. Kass, A. Kleinböhl, P. O. Hayne, D. J. McCleese, J. T. Schofield, *Jet Propulsion Laboratory, California Insitute of Technology, Pasadena, California, USA (David.M.Kass@jpl.nasa.gov)*, **N. G. Heavens**, *Department of Atmospheric and Planetary Sciences, Hampton University, Hampton, VA, USA.*

Introduction:

Martian northern spring and summer (Ls 0° to 180°) are quite different from southern spring and summer (Ls 180° to 360°) [1]. The former are cool, relatively dust free with extensive water vapor and ice clouds. The latter are warm and dusty with the regular occurrence of very large dust storms. These seasonal differences are true in both hemispheres.

The northern spring and summer are also referred to as the aphelion season [2,3] since aphelion (Ls 71°) occurs near the northern solstice (Ls 90°) and the reduced insolation due to the increased distance to the sun is a primary driver of the overall cooler seasonal climate. The low temperatures lead to an increase in equatorial water ice clouds, called the aphelion cloud belt [4]. The aphelion season is also recognized for its low inter-annual variability [4,5,6], especially in a climatological sense. There is still weather and dust storm activity during the season, especially in the mid-latitudes and polar regions [7].

Mars Climate Sounder (MCS) Observations:

MCS is an infrared 9 channel limb staring radiometer [8]. The retrieval algorithm [9,10,11] produces vertical profiles of temperature, dust and water ice extinction versus pressure. The MCS detectors have a 5 km vertical resolution on the limb, providing a half scale height resolution. The retrieved profiles generally extend from the surface to ~80 km. MCS is on the MRO orbiter in a near polar sun-synchronous orbit with a local mean solar time of 3 AM/3 PM at the equator [12].

While MCS samples multiple local times we focus on the daytime (3 pm) and nighttime (3 am) observations since they have been the most consistently acquire ones. We also focus on the retrieved temperatures at 50 Pa (~25 km) as a good representation of the lower atmosphere above the boundary layer.

A zonal mean climatology was created by binning the retrievals in 5° latitude by 2° Ls bins, separated by time of day. The MCS observations start at Ls = 110° in MY 28 and continue to the present. Thus there are observations during the northern spring and summer from 6 Mars Years (MY 28 through MY 33), so far.

Aphelion Season Climatology:

Seasonal Overturning Circulation. During the aphelion season, there are two dominant circulations [13]. The first is the equinox circulation at the beginning and end of the season. While the two equinoxes show slight differences, they are very similar in terms of the expected circulation. Figure 1 shows the thermal structure reflecting two symmetric overturning cells in the atmosphere and well developed cold polar vortices in both hemispheres.

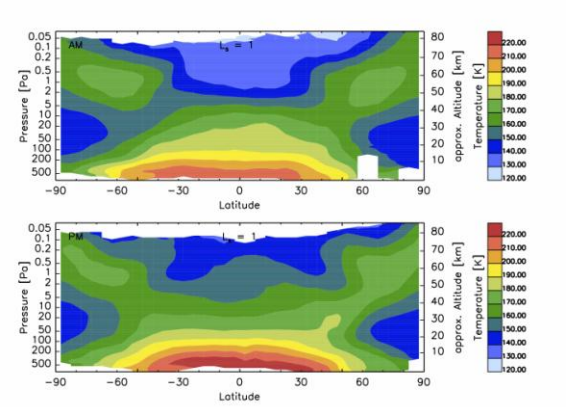

Figure 1. Zonal mean temperature cross section for Ls 0° to 2° in MY 33 from MCS retrievals. Top panel are nighttime temperatures (3 AM) while the bottom panel are daytime temperatures (3 PM).

The second dominant circulation is the northern summer solstice configuration (Ls 90°). This is illustrated in figure 2. In this case, there is a dominant cross-equatorial overturning circulation and a very strong southern winter polar vortex.

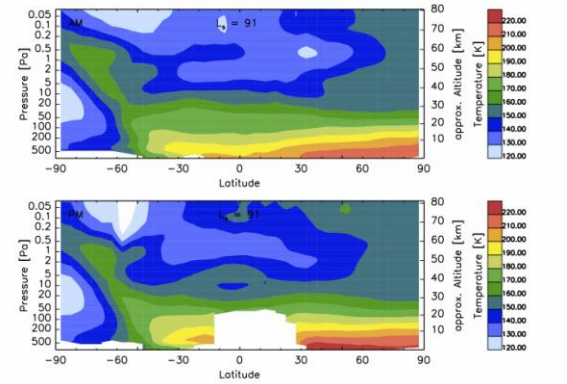

Figure 2. Same as figure 1, but Ls 90° to 92° in MY 33.

Median 50 Pa Climatology. To examine the seasonal climatology, we take the median of all of the years (with observations) for each bin and use it as

the seasonal climate. The median was selected to filter out infrequent and/or variable weather events.

Figures 3 and 4 show the daytime (3 pm) and nighttime (3 am) median climatology for northern spring and summer. The martian year starts out warm (for the aphelion season) and cools rapidly over ~45° of Ls to a minimum temperature. Despite being well before aphelion, this is followed by an overall warming trend that lasts through the rest of the season. The warming does accelerate towards the end of northern summer, especially after Ls 155°.

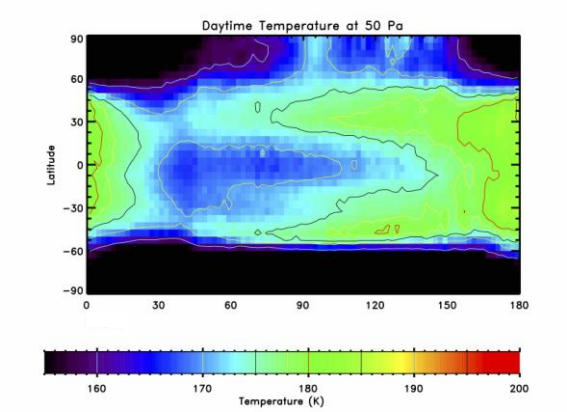

Figure 3. Daytime (3 pm) median temperature structure of northern spring and summer at 50 Pa (~25 km).

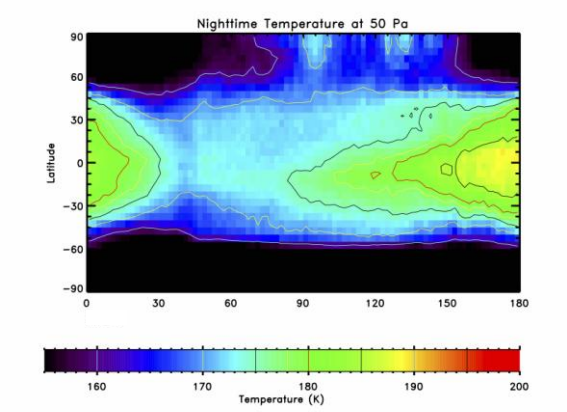

Figure 4. Same as 3, but nighttime (3 am).

The Ls 45° temperature minimum is followed by a fairly sharp (and noticeable), but modest, overall warming that occurs at the identical Ls in all MY. The change appears to be associated with the transition from the equinoctial to the solstitial circulation regime and the disappearance of the northern polar vortex. This transition is also associated with a significant change in the global structure of the diurnal thermal tide. Prior to Ls ~45°, the tide is poorly expressed at 50 Pa, but it appears at the transition (clearly seen in comparing the daytime and nighttime temperatures in Figures 3 and 4).

The more rapid warming towards the end of the season appears to be due to an increase in the amount of background atmospheric dust. However, it also coincides with the (re-)formation of the northern cold polar vortex and transition to an equinoctial circulation. The timing of the transition is very repeatable. The actual warming does vary year-to-year (see below), presumably due to the amount of dust and size of dust storms.

The southern polar vortex is well developed throughout the season. The overall latitudinal extent is constant (especially between Ls 45° and 150°). This is despite the significant changes in polar night and the growth/retreat of the seasonal frost cap [14]. The size of the vortex actually increases during the early and late periods of the season. At these times an equinoctial circulation has developed and there is a significant northern polar vortex as well.

Aphelion Season Inter-Annual Variability:

In order to examine the inter-annual variability in the climate at this season, as well as major weather events, we subtracted the median climatology from the zonal mean values for each Mars Year. This particularly reveals large scale weather events, primarily large dust storms that perturb the temperatures beyond the boundary layer. The resulting daytime maps at 50 Pa are show in figures 5 through 10.

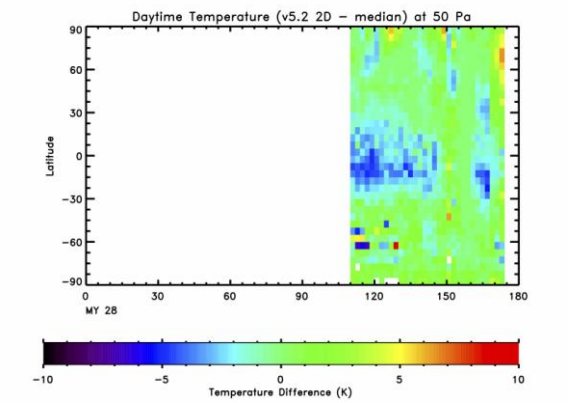

Figure 5. MY 28 zonal mean temperature deviations from the median climate for daytime observations at 50 Pa (~25 km). Note that the MCS mission started at Ls 110° of this year.

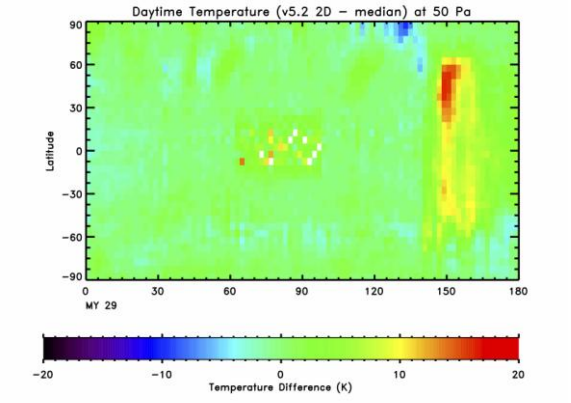

Figure 6. MY 29 zonal mean temperature deviations from the median climate for daytime observations at

50 Pa (~25 km). Note the change in scale bar.

Large Regional Dust Event (MY 29). Over the six years with MCS coverage, there is only one dust event that qualifies as a large regional-scale event capable of significantly perturbing the lower atmosphere [15]. It occurs in MY 29 (Figure 6), starting around Ls 146°, although there are some earlier perturbations in the southern hemisphere, and lasting ~25° of Ls. The strongest warming is in the northern hemisphere (the summer hemisphere), with peak temperatures of ~195 K, exceeding the zonal median by ~15 K. This is a relatively modest event compared to the ones seen in the dusty season [15]. It is longer than any of the C storms, but most dusty season storms show stronger atmospheric warming and higher peak temperatures. The difference is probably due to the reduced insolation. Likewise, the stronger northern hemisphere warming is due to the season, with the sub-solar point in the northern hemisphere.

Unlike the repeatable storms of the dusty season [15], most years do not have a large dust storm at this season. There is a moderate dust event in MY 32 (Figure 9), but the peak temperatures were only ~185 K, or ~6 K above the median (TES and THEMIS observations record two additional storms—MY 24 and MY 27—at this season).

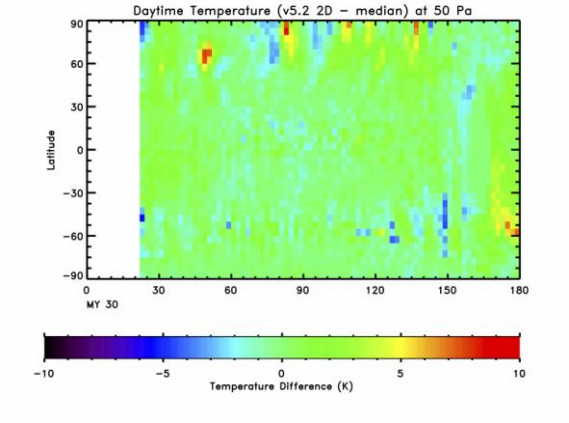

Figure 7. MY 30 (otherwise same as Figure 5).

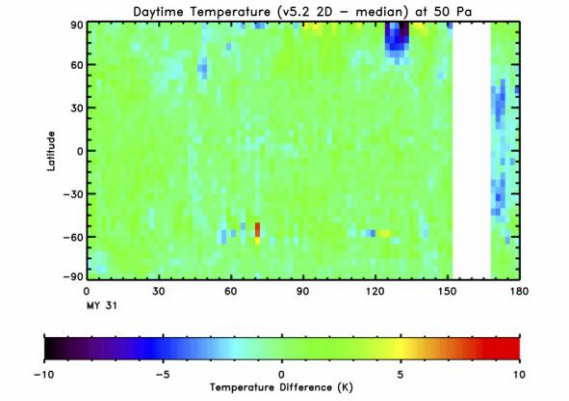

Figure 8. MY 31 (otherwise same as Figure 5).

North Polar Dust Storms. Starting around the solstice, there are sudden warming events in the northern polar region. These are driven by dust storms raised by the summer polar circulation. They continue to occur until the cold polar vortex starts to grow at around Ls 155° (dust lifting events probably continue after this point [7], but are confined close to the surface and no longer able to influence temperatures at 50 Pa). Most storms generate relatively modest warming of 5 K to 7 K although a few exceed 10 K of warming. The impact remains confined pole-ward of 60° N. At these latitudes and seasons, the storm is in polar day and thus has a warming signature in the "nighttime" data as well as the daytime.

One event is quite repeatable, occurring in all five years with MCS observations between Ls 90° and Ls 100°. Thus it shows up in the median field (Figure 3 and 4). In MY 30 it is really a series of much smaller and discrete storms, thus the cold deviations in the map.

All years (with sufficient coverage) have at least one additional storm in the same region later in the season. In a median sense, the event shows up between Ls 125° and 135°. However, this is more the overlap of a number of smaller events from about half the years. The actual timing shows up as warm features at the north pole in the deviations from the median (and the median "event" as a cold feature in the years it did not occur). MY 30 is unusual in not having any relatively long event, but instead a series of about 10 very short events throughout the season.

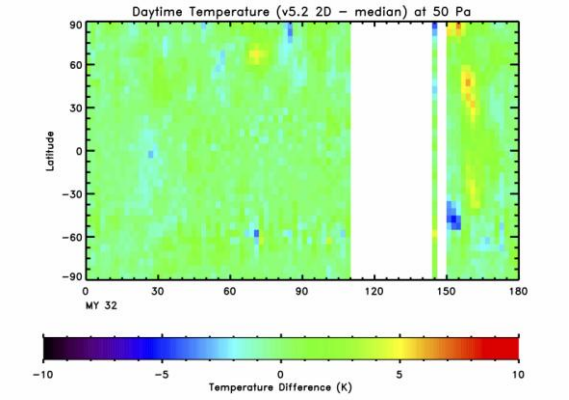

Figure 9. MY 32 (otherwise same as Figure 5).

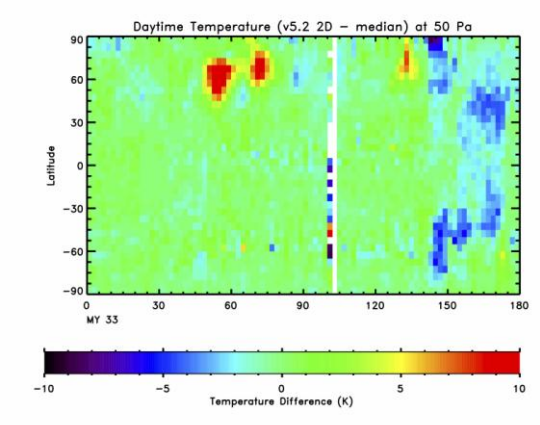

Figure 10. MY 33 (otherwise same as Figure 5).

Pre-Solstice Weather. There are very few features in the deviations prior to the solstice. This is a signature of the extreme repeatability of the season. However, there are a few apparent events. All are in the northern high latitudes, pole-ward of 45° N (but non-polar). Two events with significant warming are in MY 33 at Ls 55° and Ls 72°. There is a smaller event in MY 30, also around Ls 55°. Finally, there is a weak event in MY 32 at Ls 70°. The strong expression of these events is partly due to being on the edge of the cold polar region/vortex. Thus any northward perturbation of mid-latitude temperatures results in a strong deviation.

Conclusions:

The overall climate of the aphelion season is dominated by the transitions in overturning circulation between the equinoctial and solsticial configurations. These changes are associated with the formation/dissipation of cold (winter) polar vortices in the northern hemisphere as well as changes to the diurnal tidal structure. As previously noted [4,5,6], there is very little inter-annual variability at these seasons with cool and icy conditions dominating the climate. These conditions do change, with increased variability and dustiness starting around Ls 150°, as the atmosphere transitions back to an equinoctial configuration.

Dust activity affecting the temperature structure beyond the boundary layer is sparse and modest at this season. There is only one storm across the six years that might be classified as a large regional-scale dust event [15]. There is noticeable dust activity in the northern polar region starting around the solstice.

MCS observations spanning six Mars Years provide an excellent view of the weather and climate during the northern spring and summer season. They allow the definition of a median climate.

Acknowledgements: This work was performed at the Jet Propulsion Laboratory, California Institute of Technology, under contract with the National Aeronautics and Space Administration. © 2016, California Institute of Technology. Government sponsorship acknowledged.

References: [1] Kieffer *et al.* (1992), *Mars*, The University of Arizona Press, Tucson; [2] Smith (2004), *Icarus* 167, 148-165; [3] Liu *et al.* (2003) *JGR 108* (E8), 10.1029/2002JE001921; [4] Clancy *et al.* (2003) *JGR 108* (E9), 5098; [5] Richardson (1998) *JGR 103* (E3), 591–5918; [6] Shirley *et al.* (2015) *Icarus 251*, 26-49; [7] Cantor *et al.* (2010) *Icarus 208*, 61– 81; [8] McCleese, *et al.* (2007) *JGR, 112*, E002790; [9] Kleinböhl *et al.* (2009), *JGR 114*, E10006; [10] Kleinböhl *et al.* (2011), *JQRST 112*, 1568-1580; [11] Kleinboehl, A. et al. (2016) JQSRT, submitted; [12] Zurek and Smrekar (2007), *JGR, 112*, E05S01; [13] McCleese *et al.* (2010) *JGR, 115*, E12016; [14] Piqueux *et al.* (2015) *Icarus, 251*, 164–180; [15] Kass *et al.* (2016) *GRL 43*, 6111 – 6118.